Nanoscale

Cite this: *Nanoscale*, 2011, **3**, 3609

www.rsc.org/nanoscale

COMMUNICATION

# Au@Ag core–shell nanoparticles: efficient all-plasmonic Fano-resonance generators†

**Ovidio Peña-Rodríguez*[ab] and Umapada Pal[c]**

*Received 16th June 2011, Accepted 15th July 2011*
**DOI: 10.1039/c1nr10625b**



**Fano resonances (FR) in strongly coupled systems like a metallic dimer arise due to the coupling between the spectrally localized surface plasmon resonance (SPR) of a noble metal nanoparticle and the continuum of interband transitions of the other. Since its discovery in Au–Ag dimers, several plasmonic structures have been proposed as candidates for obtaining Fano resonances. However, most of them either are difficult to synthesize or do not generate FR signal of adequate intensity. In this paper we demonstrate that simple Au@Ag core–shell nanoparticles with typical shell thickness below 5.0 nm, which can be synthesized through a common citrate reduction method, have a Fano resonance easily detectable in the far-field.**

## Introduction

Localized surface plasmon resonances (SPR) in noble metal nanoparticles have been extensively studied in recent years. Along with enhanced light absorption, spectral tuning of the SPR by controlling the size, shape, composition and surrounding medium is essential for most applications of metal nanoparticles.[1–7] Indeed, there are so many variables that influence the SPR[8] that despite the large volume of reported works new aspects of this phenomenon are still coming out, highlighting the possibility of novel applications of these metal nanoparticles. One of the most striking examples is the all-plasmonic Fano resonance, which has become a hot research topic since its first demonstration.[9] Fano profiles are typical spectral features caused by the coupling of a discrete state with a continuum. The phenomenon was first described for a near-field coupled Au–Ag dimer, where the spectrally localized SPR of the silver nanoparticle (the discrete level) was coupled to the inter-band transitions of the gold nanoparticle (the continuum).

[a]*Centro de Microanálisis de Materiales, Universidad Autónoma de Madrid, Cantoblanco, E-28049 Madrid, Spain. E-mail: ovidio@bytesfall.com; Fax: +34 91 497 3623*
[b]*Instituto de Óptica, Consejo Superior de Investigaciones Científicas, C/Serrano 121, E-28006 Madrid, Spain*
[c]*Instituto de Física, Benemérita Universidad Autónoma de Puebla, A.P. J-48, Puebla, 72570, Mexico. E-mail: upal@sirio.ifuap.buap.mx; Fax: +52 222 229 5611*

† Electronic supplementary information (ESI) available: Experimental details and transmission electron microscopy micrographs. See DOI: 10.1039/c1nr10625b

In addition to fundamental scientific interests, Fano resonances in strongly coupled systems give rise to the so-called plasmon-induced transparency (PIT),[10] which is a phenomenon similar to the electromagnetically induced transparency, previously observed in atomic systems.[11,12] In turn, PIT has a great potential for the fabrication of sub-wavelength waveguides, low-loss metamaterials and chemical sensors.[10,13–16] Therefore, it is not surprising that, apart from the original dimer, several plasmonic structures have been proposed as candidates for generating Fano resonances.[10,13,17,18] However, despite the achieved progresses, the problem is far from being solved because most of the proposed systems share with the original structure a complexity of synthesis and/or detection that makes them impractical for most applications.

In this paper we have studied the Fano profiles of Au@Ag core–shell structures[19] with a constant core size and different shell thicknesses. Firstly, a theoretical analysis was performed by combining classical Mie calculations[20–22] with a plasmon hybridization analysis. Moreover, we synthesized the core–shell structures, and their optical responses were in good agreement with the theoretical predictions. Optical responses of the nanostructures were calculated using bulk dielectric functions of Ag and Au,[23] after applying the usual size correction;[24] the refractive index of the surrounding medium was fixed at 1.33 (water). Generation of clear and detectable Fano resonance has been demonstrated in Au@Ag structures, which are much simpler in shape than previously proposed ones, and can be synthesized through simple chemical reduction techniques.

## Procedure

Mie theory[20,21] is one of the preferred methods for studying light scattering by small particles,[25] it was originally developed for solid spheres and later extended for bi- and multi-layered spheres.[26–28] However, even if one can easily calculate the optical responses of such low-dimensional structures using Mie theory, it is often very difficult to understand the origin of the observed resonances in systems such as aggregates or particles with complex shapes. Fortunately, this problem could be overcome using the theory of plasmon hybridization.[29] This recent approach is a complementary, mainly qualitative method, where the characteristics of the SPR can be explained in terms of the interactions between the plasmons of metallic nanostructures of simpler shapes.

Plasmon hybridization in a core–shell metallic nanoparticle (Fig. 1a) can be rationalized from that occurring in a

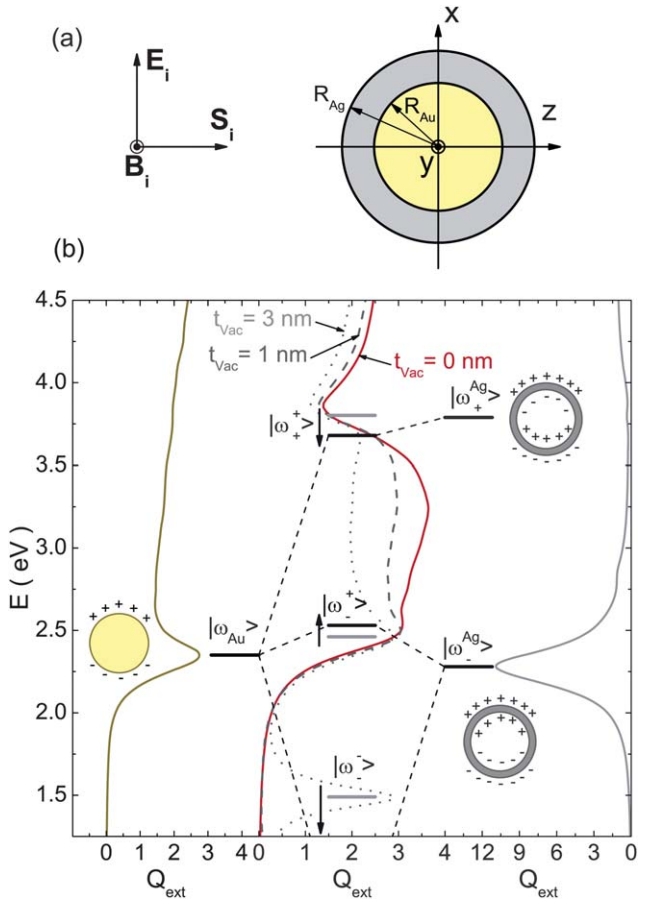


**Fig. 1** Schematic representation of a core–shell nanoparticle (a) and its corresponding energy diagram, representing plasmon hybridization (b).

metal–dielectric–metal structure.[30–32] For example, lets consider a Au–vacuum–Ag system with thicknesses ($t_{Au}$, $t_{Vac}$, $t_{Ag}$) = (20, 3, 5) nm (dotted gray line). The response of this particle can be interpreted as the interaction between the primitive plasmon mode of a solid Au sphere and the plasmon modes of the nanoshell. Three hybridized modes are obtained in this case, the energy mode $|\omega_-^-\rangle$ ($|\omega_-^+\rangle$) corresponds to the antisymmetric (symmetric) coupling between the symmetric plasmon resonance modes of the silver ($|\omega_-^{Ag}\rangle$) nanoshell and the sphere plasmon. The coupling between the higher energy antibonding mode of the outer nanoshell and the nanosphere plasmon modes is very weak and only one hybridized mode is produced in this case ($|\omega_+^+\rangle$).

Now, as we decrease the thickness of the intermediate layer (dashed gray line), several phenomena occur; the most important of these is a dramatic red shift (accompanied by a significant decrease in intensity) of the $|\omega_-^-\rangle$ energy mode. Finally, as the intermediate dielectric layer disappears (red continuous line), the bonding mode vanishes, leaving only the two highest energy modes. These last two modes are also slightly shifted when the thickness of the intermediate layer is varied, but their intensities remain largely unaffected. Perhaps due to these small shifts of the remaining hybridized plasmons in a metallic core–shell structure, they have received little attention, compared with conventional nanoshells (*i.e.*, the ones with dielectric cores). However, the similarity of this phenomenon with the one occurring in a dimer makes the core–shell structure a natural candidate for producing Fano resonances.

The $|\omega_-^+\rangle$ mode of the metallic core–shell corresponds to the two dipole moments moving in phase (symmetric electric fields), while the $|\omega_+^+\rangle$ one corresponds to the negative parity of the dipoles (antisymmetric fields). Strengthening the analogy with the dimer, if the core material is the same as that of the shell (solid sphere) then the net dipole moment of the $|\omega_+^+\rangle$ mode is zero and therefore it can not be excited by light (dark plasmon), in contrast to the $|\omega_-^+\rangle$ (bright) plasmon. On the other hand, for a core–shell structure, the symmetry is broken, and consequently, the $|\omega_+^+\rangle$mode can also be excited. It should be noted that for a thick Ag layer the above explanation fails to describe the optical response of the core–shell structure (*e.g.*, for the structure with $R_{Au}$ = 20 nm and $t_{Ag}$ = 10 nm) because the contribution of silver is so strong that the SPR obtained is basically that of a pure silver particle, except for the width, which is higher due to the energy dissipation in the gold core.

Experimentally, the Au@Ag core–shell NPs were fabricated though successive reduction of Au and Ag ions using sodium citrate and ascorbic acid as reducing agents. First the Au NPs of about 18 nm average size were prepared by reducing the $Au^{3+}$ ions by sodium citrate solution at 90 °C. Using these Au NPs as seed, $Ag^{3+}$ ions were reduced over them at the same temperature, using sodium citrate and ascorbic acid as reducing agents (see ESI† for synthesis details). To obtain the NPs of different shell thicknesses, the volumetric ratio between the $Ag^{3+}$ ion solution and the Au seed solution was varied. For microscopic observation of the synthesized nanoparticles, they were dispersed over carbon coated microscopic copper grids and inspected using a JEOL 2010 FEG transmission electron microscope operating at 200 keV.

## Results and discussion

If the real dielectric functions of the metals are used for the calculation of extinction efficiency ($Q_{ext}$) then it is impossible to directly see the weak antibonding mode, mainly because it falls in the region of the interband transitions of gold. For that reason, we performed the first calculations (Fig. 2) by using Drude's dielectric function,[21] $\varepsilon(\omega) = \varepsilon_\infty - \omega_p^2/(\omega^2 + i\omega\Gamma)$; where $\varepsilon_\infty$ is the high-frequency limit dielectric constant, $\omega_p$ is the Drude plasma frequency and $\Gamma$ is the damping constant. For the calculations, we used the parameters

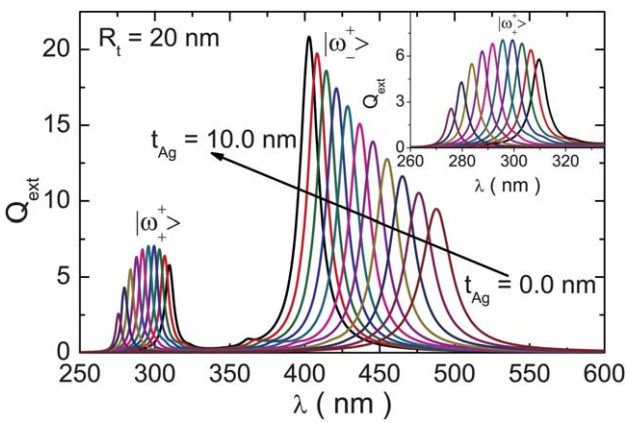


**Fig. 2** Simulated extinction efficiency, calculated using Drude's dielectric functions, for a core–shell nanoparticle having $R_t$ = 20.0 nm, while the thickness of the shell layer is varied in between 0.0 and 10.0 nm. For clarity, the antibonding mode is amplified in the inset.

$\omega_p = 9.1721$ eV, $\varepsilon_\infty = 4.039$, and $\Gamma = 0.0207$ eV ($\omega_p = 9.0146$ eV, $\varepsilon_\infty = 8.7499$, and $\Gamma = 0.0691$ eV) for Ag (Au), obtained from the best fit of the experimental dielectric functions[23] for wavelengths above 400 nm (600 nm); *i.e.*, in the energy region below interband transitions. It should be noted that the parameters obtained for silver match with those reported by Mirin, Bao and Nordlander.[33] A fixed nanoparticle radius of 20.0 nm was used for the calculations and the thickness of the shell layer was varied between 0.0 and 10.0 nm. The development of both the symmetric and asymmetric modes can be seen in Fig. 2; the former is more intense than the later, as expected. The $|\omega_-^+\rangle$ mode blue-shifts when the thickness of the silver layer is increased, owing to the blue-shift of the $|\omega_-^{Ag}\rangle$ energy mode. Similarly, the $|\omega_+^+\rangle$mode is red-shifted due to the red-shift of the $|\omega_-^{Ag}\rangle$ mode.

The extinction efficiency was also calculated for nanoparticles with a core radius of 20.0 nm (Fig. 3a) and 80.0 nm (Fig. 3b), using their real dielectric functions. In both cases, thickness of the shell layer was varied between 0.0 and 10.0 nm. There was no trace of the $|\omega_+^+\rangle$ SPR for the smaller thicknesses of the Ag shell. However, a Fano profile around 330 nm could be clearly seen in the spectra. As the thickness of the silver layer was increased, the Fano resonance profile was gradually hidden by the shielding produced by the shell and the increase in intensity of the antibonding SPR mode, complicating its far-field detection. The effect was almost the same for both sizes tested, despite the differences between their other spectral features. The Fano resonance is located in the same region where the narrow $|\omega_+^+\rangle$mode appears (Fig. 2), confirming that it has been

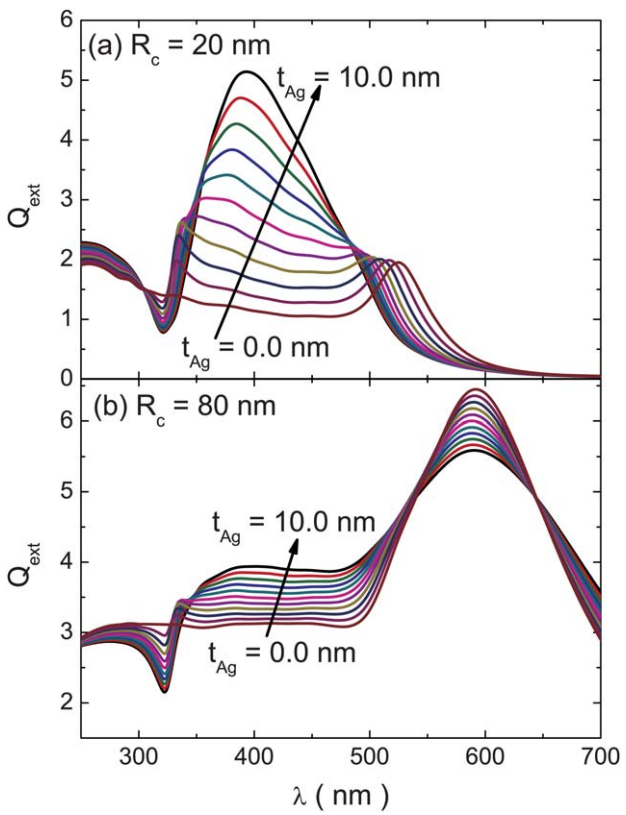


**Fig. 3** Simulated extinction efficiency, calculated using the real dielectric functions, for core–shell nanoparticles having $R_{Au} = 20.0$ nm (a) and $R_{Au} = 80.0$ nm (b). In both cases the thickness of the shell layer is varied in between 0.0 and 10.0 nm.

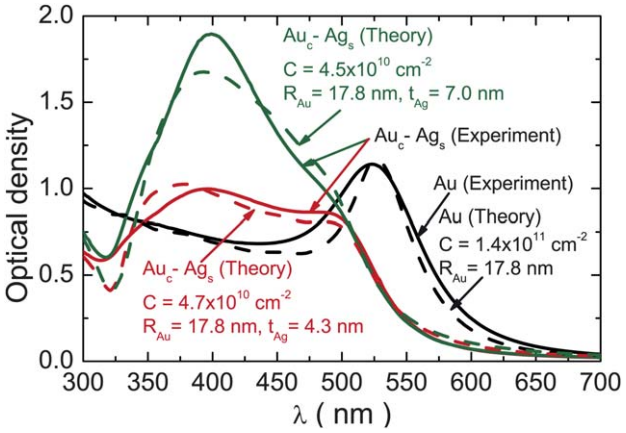


**Fig. 4** Experimental optical density of Au nanoparticles (seed, black continuous line) and the same particles covered by either thin (red continuous line) or thick (green continuous line) Ag shells. Simulated optical densities (dashed lines) are in good agreement with the experimental values.

induced by the near-field coupling between the continuum of inter-band transitions of gold (core) and the discrete $|\omega_+^+\rangle$ mode of the particle. An interesting effect observed in Fig. 3 is that the position of the FR barely changes with the variations of silver layer thickness, unlike what is observed in Fig. 2. This can be explained by the presence of the silver interband transitions from 3.87 eV (320 nm) onwards, which produce a strong damping of the $|\omega_+^+\rangle$ mode, not permitting the FR position to be shifted to higher energies. It should be noted that, unlike what occurs in the symmetrical dimer, the Fano resonance produced in these structures is detectable in the far-field, because it is not hidden by the weak antibonding SPR. The only drawback of this type of structures is that the silver layer must be very thin; this is probably the unique reason the phenomenon has not been reported yet experimentally. However, as we demonstrate, fabrication of these structures using conventional synthesis methods is quite possible.

For the experimental verification of the previous results, two different kinds of Ag shells ($t_{Ag} \approx 4$ and 7 nm) were grown over nearly monodisperse Au seed particles (~4.7% size dispersion) with an average size of about 18 nm (Fig. S1†). The appearance of the Fano resonance in their absorption spectra is clearly illustrated in Fig. 4. The absorption spectrum of the gold cores (black continuous line) is strongly modified by the thin silver layer (red continuous line) because a clear Fano resonance appears around 340 nm, as predicted by our theoretical calculations. For the thicker Ag shell, the FR is less visible (green continuous line) due to the stronger SPR. The experimental absorption spectra of the two sets of core–shell particles could be fitted well (dashed lines) considering a simple structure with a core radius, $R_{Au}$ of 17.8 nm and shell-layer thickness, $t_{Ag}$, of either 4.3 nm or 7.0 nm. However, it should be noted that those values are just approximate, since we did not consider the dispersions in shape and size of either the Au cores or the Ag shells in our fits.

## Conclusions

In this work we have demonstrated that Au@Ag core–shell structures with a thin silver layer (typically, $t_{Ag} < 5$ nm) produce a well defined and measurable Fano profile. The size of the Au

core particles does not significantly affect the position or intensity of the FR. However, controlling the thickness of the Ag shell is critical for obtaining a FR measurable in the far-field. While the synthesis of this type of structure presents some challenges (arising from the difficulty of obtaining a thin, uniform silver shell), the use of a very common synthesis method like citrate-reduction is enough for this task. The proposed configuration is a very advantageous alternative to the systems where the Fano resonances have been achieved to date, surpassing them in both simplicity and ease of detection of the optical response.

## Notes and references


1 J. Z. Zhang, *J. Phys. Chem. Lett.*, 2010, **1**, 686–695.
2 L. R. Hirsch, R. J. Stafford, J. A. Bankson, S. R. Sershen, B. Rivera, R. E. Price, J. D. Hazle, N. J. Halas and J. L. West, *Proc. Natl. Acad. Sci. U. S. A.*, 2003, **100**, 13549–13554.
3 P. Alivisatos, *Nat. Biotechnol.*, 2004, **22**, 47–52.
4 L. R. Allain and T. Vo-Dinh, *Anal. Chim. Acta*, 2002, **469**, 149–154.
5 D. Ricard, P. Roussignol and C. Flytzanis, *Opt. Lett.*, 1985, **10**, 511–513.
6 L. R. Hirsch, J. B. Jackson, A. Lee, N. J. Halas and J. L. West, *Anal. Chem.*, 2003, **75**, 2377–2381.
7 C. Sönnichsen and A. P. Alivisatos, *Nano Lett.*, 2005, **5**, 301–304.
8 K. L. Kelly, E. Coronado, L. L. Zhao and G. C. Schatz, *J. Phys. Chem. B*, 2003, **107**, 668–677.
9 G. Bachelier, I. Russier-Antoine, E. Benichou, C. Jonin, N. Del Fatti, F. Vallée and P.-F. Brevet, *Phys. Rev. Lett.*, 2008, **101**, 197401.
10 S. Mukherjee, H. Sobhani, J. B. Lassiter, R. Bardhan, P. Nordlander and N. J. Halas, *Nano Lett.*, 2010, **10**, 2694–2701.
11 K.-J. Boller, A. Imamolu and S. E. Harris, *Phys. Rev. Lett.*, 1991, **66**, 2593.
12 M. Fleischhauer, A. Imamoglu and J. P. Marangos, *Rev. Mod. Phys.*, 2005, **77**, 633.
13 N. A. Mirin, K. Bao and P. Nordlander, *J. Phys. Chem. A*, 2009, **113**, 4028–4034.
14 J. B. Lassiter, H. Sobhani, J. A. Fan, J. Kundu, F. Capasso, P. Nordlander and N. J. Halas, *Nano Lett.*, 2010, **10**, 3184–3189.
15 J. A. Fan, C. Wu, K. Bao, J. Bao, R. Bardhan, N. J. Halas, V. N. Manoharan, P. Nordlander, G. Shvets and F. Capasso, *Science*, 2010, **328**, 1135–1138.
16 N. Liu, T. Weiss, M. Mesch, L. Langguth, U. Eigenthaler, M. Hirscher, C. Sönnichsen and H. Giessen, *Nano Lett.*, 2010, **10**, 1103–1107.
17 N. Verellen, Y. Sonnefraud, H. Sobhani, F. Hao, V. V. Moshchalkov, P. V. Dorpe, P. Nordlander and S. A. Maier, *Nano Lett.*, 2009, **9**, 1663–1667.
18 O. Peña-Rodríguez, U. Pal, M. Campoy-Quiles, L. Rodríguez-Fernández, M. Garriga and M. I. Alonso, *J. Phys. Chem. C*, 2011, **115**, 6410–6414.
19 Y. Kim, R. C. Johnson, J. Li, J. T. Hupp and G. C. Schatz, *Chem. Phys. Lett.*, 2002, **352**, 421–428.
20 G. Mie, *Ann. Phys.*, 1908, **330**, 377–445.
21 C. F. Bohrenand D. R. Huffman, *Absorption and Scattering of Light by Small Particles*, Wiley-Interscience, 1998.
22 O. Peña and U. Pal, *Comput. Phys. Commun.*, 2009, **180**, 2348–2354.
23 P. B. Johnson and R. W. Christy, *Phys. Rev. B: Solid State*, 1972, **6**, 4370–4379.
24 O. Peña, U. Pal, L. Rodríguez-Fernández and A. Crespo-Sosa, *J. Opt. Soc. Am. B*, 2008, **25**, 1371–1379.
25 U. Kreibig and M. Vollmer, *Optical Properties of Metal Clusters*, Springer, 1st edn, 1995.
26 A. L. Aden and M. Kerker, *J. Appl. Phys.*, 1951, **22**, 1242–1246.
27 J. Wait, *Appl. Sci. Res., Sect. B*, 1963, **10**, 441–450.
28 R. Bhandari, *Appl. Opt.*, 1985, **24**, 1960–1967.
29 E. Prodan, C. Radloff, N. J. Halas and P. Nordlander, *Science*, 2003, **302**, 419–422.
30 D. Wu and X. Liu, *Appl. Phys. B: Lasers Opt.*, 2009, **97**, 193–197.
31 R. Bardhan, S. Mukherjee, N. A. Mirin, S. D. Levit, P. Nordlander and N. J. Halas, *J. Phys. Chem. C*, 2010, **114**, 7378–7383.
32 O. Peña-Rodríguez and U. Pal, *Nanoscale Res. Lett.*, 2011, **6**, 279.
33 E. Prodan, P. Nordlander and N. J. Halas, *Nano Lett.*, 2003, **3**, 1411–1415.


 